# Tracking Divers

## *An Autonomous Marine Surface Vehicle to Increase Diver Safety*

By Nikola Mišković, Đula Nađ, and Ivor Rendulić

Diving is a high-risk activity due to the hazardous environment, dependence on technical equipment for life support, complexity of underwater navigation, and limited monitoring from the surface. This article describes a new concept of using an autonomous surface vehicle (ASV) as a private satellite that tracks divers, thus significantly increasing diving safety. Since the vehicle is above the diver at all times, acoustic communication with the diver interface in the form of an underwater tablet is more efficient and robust, which enhances diver navigation and enables reliable monitoring from the surface. This article focuses on a diver-tracking control structure that uses a diver motion estimator to determine diver position, even in cases when acoustic position measurements are not available.

Conducting experiments with divers presents a challenge due to uncertainties, such as those introduced by the environment, unmodeled dynamics, acoustic sensors, and divers themselves (e.g., the emission of air bubbles). A step-by-step experimental plan, which includes a virtual diver (VD), an underwater remotely operated vehicle (ROV), and a human diver, allows the identification of different uncertainties. The results show that the mean tracking error with a VD (influenced only by the environment and unmodeled dynamics) is around 0.5 m; with an ROV (including the influence of acoustic sensor), it is around 1 m; and with a human diver, it is around 1.8 m. These data are validated against ground-truth video imagery.

*Digital Object Identifier 10.1109/MRA.2015.2448851*
*Date of publication: 11 September 2015*





1070-9932/15©2015IEEE

## Mitigating Hazards to Divers

Scuba diving activities, whether they are recreational, scientific, or technical, are classified as high risk due to

- the unpredictable, dangerous, and unfamiliar environment constantly under influence of external disturbances
- the dependence on the technical equipment that ensures life support
- the health consequences that diving can have on a diver.

Diver safety is one of the major concerns of the diving industry. The Divers Alert Network, one of the largest training agencies in the world, identified the most significant triggering events that lead to fatalities as air loss, entrapment or entanglement, gear issues, rough water, and buoyancy issues. In 20% of scuba diving fatalities, the initial triggering event could not be determined.

One significant cause of accidents during diving is the loss of consciousness in the water. The final outcome is very often the same—drowning. Nitrogen narcosis is a state when a diver seems perfectly fine at first but is intoxicated, if not unconscious, and cannot make sane decisions. An inexperienced dive buddy may not even notice nitrogen narcosis. It has been reported by experienced divers that, while under this state, their buddies seemed perfectly fine until they started some unexpected behavior, such as separating from the buddy, not following previously agreed mission plans, changing depth rapidly, or even taking their masks off. Once this state is recognized (which is a challenge for an inexperienced dive buddy), the simple act of attracting the attention of the diver can snap him or her out of this state, which, if left unattended, may have catastrophic consequences. Even though diver safety risks are commonly minimized by diving in groups, or at least in a pair with a buddy, statistics show that 40% of the fatalities take place during a period of buddy separation and 14% involve declared solo dives, meaning that more than 50% of accidents happened while the divers were not accompanied.

Diver safety is seriously jeopardized during diving activity not only because of unpredictable underwater scenarios but also because of diver invisibility to surface vessels. Currently, diving areas are marked using passive buoys with international dive flags that serve as indicators for man-operated surface vessels to avoid the area. Unfortunately, these markings are often disregarded by surface vessels. The diver's area of operation can be increased if the diving buoy is linked to the diver via a cable [1]—but this solution is unacceptable for deep and/or long dives due to possible entanglement, drag, and cumbersomeness.

Even though diver safety is the most significant issue, diving activities are also significantly hampered by the lack of navigation capabilities and communication with the surface. Underwater navigation poses a challenge even for experienced divers. Gravity compromised by buoyancy, limited visibility, and lack of global navigation satellite system reception jeopardize divers' activities as well as safety underwater. Classical techniques for underwater navigation, such as referencing according to the sun, a compass, or underwater features, are imprecise, tedious, and require concentration and experience.

Current technological solutions enable determining the position of the diver relative to the surface station by using acoustic-based technology. These systems, which rely on static transmitters/receivers, exhibit serious performance deterioration due to acoustic multipath effects when the diver is distanced from the ship [2]. For the same reason, communication between the diver and the surface is an important issue and can compromise diver monitoring from the surface if interrupted. Reliable communication is important to diving supervisors, who monitor the progress of diving operations, as well as the divers themselves, who appreciate monitoring as a way of increasing their safety during dives. Current communication systems, as in the case of navigation, are not appropriate at larger distances (due to multipath) or in cases when obstacles are present between the diver and the base station.

**A vertical acoustic communication channel of minimal distance is formed, ensuring reliable communication.**

### *Concept*

This article proposes a new concept for dealing with the aforementioned major diving challenges by using an omnidirectional ASV with the ability to follow the diver and act as a private satellite, thus significantly increasing diver safety, alleviating underwater navigation difficulties, and enabling monitoring from the surface. Since the ASV is tracking the diver at all times, i.e., keeping its position above the diver, as shown in Figure 1, the following set of functionalities is accomplished.

- Since the ASV carrying the international dive flag is always above the diver, it expands the diver's safe underwater operation area. There is no need for the conventional marking of the diver area by using static buoys, and physical tethering with the buoy is avoided since the ASV uses acoustic localization of the diver for tracking.
- A vertical acoustic communication channel of minimal distance is formed, ensuring reliable communication and avoiding multipath problems. This also allows reliable transmission of global positioning system (GPS) coordinates to the diver, thus providing the diver with absolute GPS coordinates on his or her tablet.
- The diving supervisor at the surface has reliable data about the diver's position, and reliable communication between the diver and the diving supervisor is established through the vertical communication channel, thus significantly increasing reactivity in case of danger.

### *Related Work*

The research area of diver–robot cooperation is very young, but, with the increased demand in autonomous marine robotics, the

need for interaction with divers arises. Even though human divers today are increasingly being replaced with autonomous underwater vehicles in tedious tasks such as mapping and searching, there are still many applications that require a human presence underwater. These applications are mostly related to unconventional, nonrepetitive tasks such as underwater interventions.

Underwater ROVs have been commonly used in tandem with divers, mostly for the purpose of monitoring divers from the surface. However, the use of autonomous marine vehicles has taken place only recently. The list of autonomous underwater robots used for diver–robot applications is fairly short:

- AquaRobot [3], developed at McGill University, initially used as an amphibious robot for exploring underwater environments, was used to track divers based on visual detection of their motion [4].
- The BUDDY AUV, developed for the purposes of the European project Cognitive Autonomous Diving Buddy (CADDY, http://caddy-fp7.eu/), is the first AUV for interacting with divers by using an underwater touchscreen.

Tracking and navigating divers using ASVs was first addressed by the European project Cooperative Cognitive Control for Autonomous Underwater Vehicles [5]. A fleet of three ASVs was deployed, and successful diver-tracking and -guidance experiments were performed by using single range measurement from the vehicles [6]. This project was a stepping stone toward the CADDY project, under which the results presented in this article were obtained. It should be mentioned that other efforts have been made toward robot–diver interaction, such as [7]; however, these were done only in the simulation environment, without addressing the issues of diver detection or localization. While using acoustic positioning systems to localize divers is the most straightforward method, visual [4], [8] and sonar [9] detection can be found in the literature.

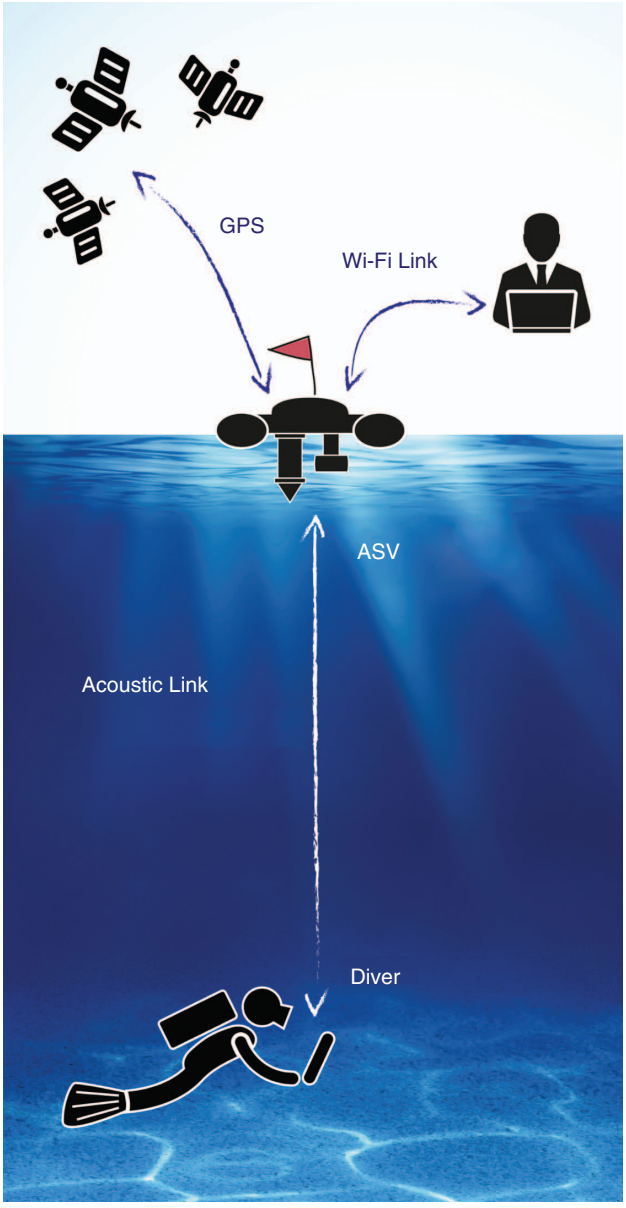


**Figure 1.** A novel concept for increasing diver safety: an autonomous surface platform, PlaDyPos, serving as the diver's private satellite and interfacing with the diver through an underwater tablet.

### *Contributions*

The main contributions of this article are both in technical and control aspects as well as benchmarking and experiment design and execution. The first contribution is the development of the diver-tracking system consisting of an autonomous surface marine vehicle and an underwater diver interface used for two-way communication between the diver and the surface vehicle. The complete system is described in the next section. The second contribution is the onboard diver-tracking algorithm that uses intermittent acoustic diver position measurements fused with a diver motion estimator. The models, control, and tracking algorithms were initially described in a previous paper by the authors [10], but they are also included in this article for completeness. The third contribution is the design of a benchmark scenario with associated metrics for human–robot tracking performance measurement in the underwater environment. The benchmark scenario enables replicability of experiments in real conditions with human divers. Finally, the fourth contribution is the design and execution of an experimental plan that allows the identification of uncertainties introduced by the human diver, environment, unmodeled dynamics, and acoustic sensors by using tracking performance metrics.

## Diver–Robot System Description

The overall diver-tracking system presented in this article consists of three main components: 1) the diver-tracking marine ASV, 2) the diver, and 3) an underwater tablet carried by the diver, serving as the diver's interface. The components are described in the following section, while the communication scheme between them is shown in Figure 2.

### *ASV–PlaDyPos*

The ASV PlaDyPos (named after its initial purpose as a platform for dynamic positioning), Platform for Dynamic

Positioning (PlaDyPos) acts as an ASV and carries the international flag marking underwater activity. It has four thrusters in an "X"-shaped configuration, allowing omnidirectional motion, i.e., motion in the horizontal plane under any orientation. PlaDyPos, shown in Figure 3, has been developed at the Laboratory for Underwater Systems and Technologies at the University of Zagreb Faculty of Electrical Engineering and Computing, Croatia, and it is 0.35-m high, 0.707-m wide and long, and weighs approximately 25 kg. The control computer (isolated from environmental disturbances inside the platform hull) is in charge of performing control and guidance tasks (dynamic positioning, path following, and diver following) and all the data processing. Apart from the compass, batteries, and central processing units the PlaDyPos payload relevant to the diver-tracking experiments consists of

- a ublox Neo 6P GPS for determining position and, indirectly, the diver position in the horizontal plane
- a Tritech MicroNav ultrashort baseline (USBL) used to determine the position of the diver relative to the vehicle, with integrated acoustic modem
- a Bullet M2 wireless modem used for two-way communication with the ground station, thus making PlaDyPos a router from the diver to the surface station where the diving supervisor is stationed.

The USBL, shown in Figure 3(b), is used simultaneously for localization and two-way data transmission via an acoustic link (the second modem is mounted on the diver). While diver localization is the main topic of interest in this article, it should be mentioned that the acoustic link can be used to transmit messages as well as diver position based on USBL and GPS measurements from the vehicle.

### *Diver*

The diver is mounted with an acoustic modem that is used for localization on board the surface vehicle as well as to communicate with the modem on the surface vehicle. As shown in Figure 2, the diver-mounted acoustic modem is connected to the RS232-Bluetooth converter, which allows transmission of the data via Bluetooth link. Our experiments have shown that Bluetooth communication has a range of about 15 cm underwater, which allows the diver-mounted Bluetooth module to establish a connection with another Bluetooth device in close proximity, such as the one on the tablet in the waterproof casing.

**The overall diver-tracking system presented in this article consists of three main components.**

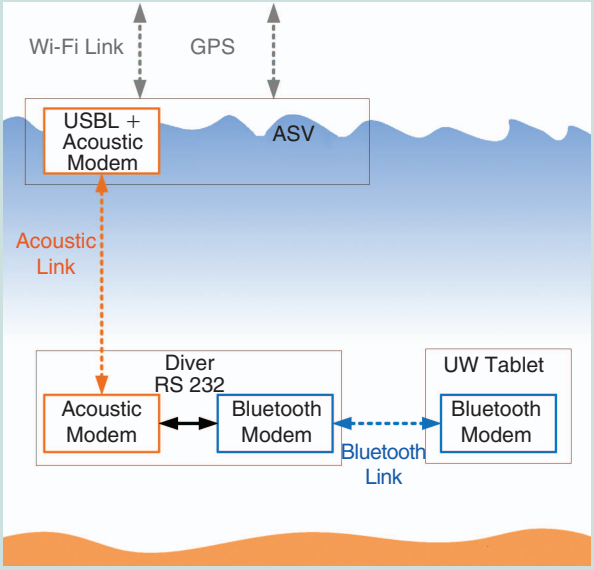


**Figure 2.** A schematic representation of the communication structure between the surface robot, the diver, and the underwater tablet. The ASV is linked to the diver-mounted modem via acoustic link, while the modem communicates via RS232 with the Bluetooth modem that connects to the underwater tablet through the Bluetooth connection that has proved to work underwater at short distances.

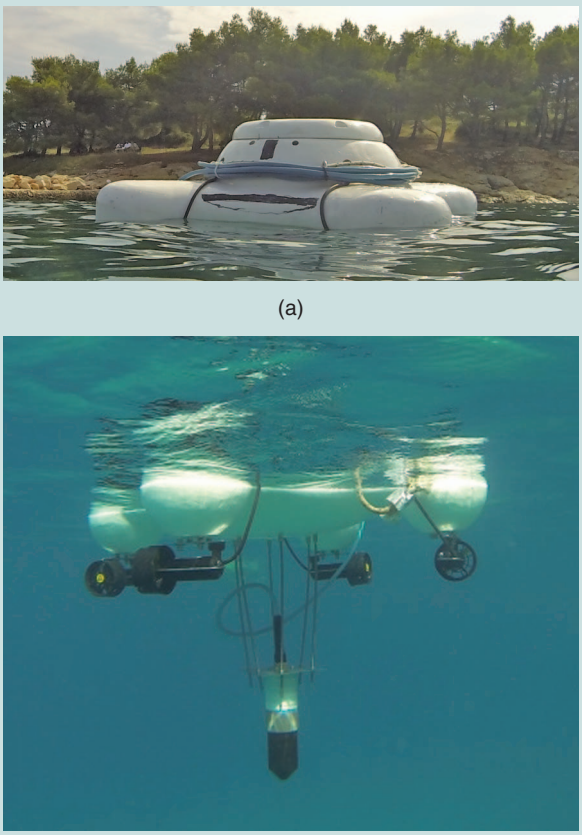


**Figure 3.** The diver-tracking ASV PlaDyPos viewed from (a) above and (b) below. The USBL mounted on the bottom of the hull is used to communicate and determine the position of the diver-mounted modem via acoustic link. This configuration makes PlaDyPos a router between the diver and the surface station where the diving supervisor is stationed.

### *Underwater Diver Interface*

The diver carries an underwater interface (a commercially available tablet) sealed in a custom-made waterproof casing that has been tested in a pressure chamber for depths up to 50 m. Larger depths can be achieved but at the expense of a more robust and cumbersome design. The diver-mounted Bluetooth modem is placed on the waterproof casing, enabling a Bluetooth connection with the tablet without compromising the structural integrity of the casing itself. A tablet with an inductive touchscreen is integrated in the overall system, allowing the diver to send feedback to the surface platform via an acoustic modem. A commercially available stencil has been modified to preserve touchscreen functionalities at rated depths. An Android application that has been developed for this purpose has the following set of functionalities.

- The diver position transmitted from PlaDyPos is directly overlayed on an integrated Google map, allowing the diver absolute localization, as is possible on dry land where a GPS signal is present.
- Two-way communication with the surface in the form of predefined or custom short messages is enabled, as well as a single-touch alert message in case of hazards.
- Waypoints, tracks, or marked areas can be sent from the surface and displayed directly on the diver's tablet, and thus the diver can visit areas of interest sent from the ground station.

A diver carrying the tablet in the underwater casing on dry land during one of the experiments in Croatia is shown in Figure 4.

**Figure 4.** A diver with the underwater tablet preparing to start the experiments. The underwater casing, rated for depths up to 50 m, allows touchscreen functionality when using tablets with inductive screens. The tablet is linked to the surface via the acoustic modem mounted on the diving tank.

## Mathematical Modeling

### *Modeling the ASV*

#### Dynamic Model

Following the notation shown in Figure 5, a dynamic model of the platform in the horizontal plane can be described using the velocity vector $\boldsymbol{\nu} = [u \;\; v \;\; r]^T$, where $u, v$, and $r$ are the surge, sway, and yaw speed, respectively; and the vector of actuating forces and moments acting on the platform $\boldsymbol{\tau} = [X \;\; Y \;\; N]^T$, where $X, Y$ are the surge and sway forces and $N$ is the yaw moment [11]. Both vectors are defined in the body-fixed (mobile) coordinate frame. The uncoupled dynamic model in the horizontal plane is given with (1), where $\mathbf{M}$ is a diagonal matrix with mass and added mass terms, and $\mathbf{D}(\boldsymbol{\nu})$ is a diagonal matrix consisting of nonlinear hydrodynamic damping terms

**Conducting experiments with divers presents a challenge due to uncertainties.**

$$\mathbf{M}\dot{\boldsymbol{\nu}} = -\mathbf{D}(\boldsymbol{\nu}) + \boldsymbol{\tau}. \tag{1}$$

Since the platform is designed to be symmetrical with respect to the $x$ and $y$ axes in the body fixed frame, the following forms of the two matrices are adopted: $\mathbf{M} = \text{diag}(\alpha_u, \alpha_u, \alpha_r)$, $\mathbf{D}(\boldsymbol{\nu}) = \text{diag}(\beta_u(u), \;\; \beta_u(v), \;\; \beta_r(r))$.

#### Kinematic Model

The kinematic equations for the platform motion in the horizontal plane on the sea surface is given with (2), where $x$ and $y$ are the position and $\psi$ is the orientation of the platform in the Earth-fixed coordinate frame. The rotation matrix $\mathbf{R}(\psi)$ is given with

$$\begin{bmatrix} \dot{x} \\ \dot{y} \\ \dot{\psi} \end{bmatrix} = \begin{bmatrix} \mathbf{R}(\psi) & 0 \\ \mathbf{0}_{[1\times 2]} & 1 \end{bmatrix} \begin{bmatrix} u \\ v \\ r \end{bmatrix} \tag{2}$$

$$\mathbf{R}(\psi) = \begin{bmatrix} \cos\psi & -\sin\psi \\ \sin\psi & \cos\psi \end{bmatrix}. \tag{3}$$

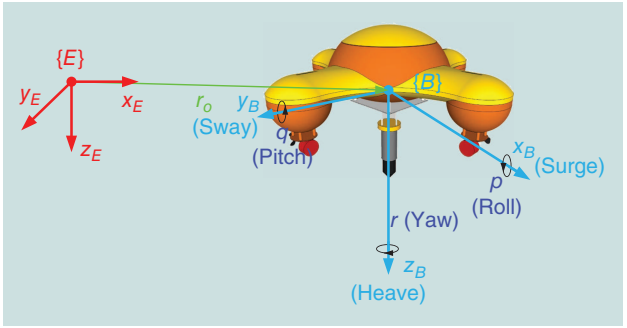


**Figure 5.** The body-fixed and Earth-fixed coordinate frames attributed to the ASVs. This notation is usually used in marine vehicles, as described in [11].

The platform is overactuated, i.e., it can move in any direction in the horizontal plane by modifying the surge and sway speed, while attaining arbitrary orientation.

### Actuator Allocation

The actuator allocation matrix $\Phi$ gives the relation between the forces exerted by the thrusters $\boldsymbol{\tau}_\mathbf{i} = [\tau_1 \ \ \tau_2 \ \ \tau_3 \ \ \tau_4]^T$ and the forces and moments $\boldsymbol{\tau}$ acting on the rigid body. The actuator configuration of the autonomous surface platform for diver tracking is given in Figure 6, where $\delta = 45^\circ$. The allocation matrix is given with

$$\boldsymbol{\tau} = \underbrace{\begin{bmatrix} \cos 45^\circ & \cos 45^\circ & -\cos 45^\circ & -\cos 45^\circ \\ \sin 45^\circ & -\sin 45^\circ & \sin 45^\circ & -\sin 45^\circ \\ D & -D & -D & D \end{bmatrix}}_{\Phi} \boldsymbol{\tau}_\mathbf{i}. \tag{4}$$

### The Diver Model

Determining a simple dynamic model of a diver is practically impossible. For the specific case of the ASV tracking a diver from the surface, a kinematic model of the diver projection on the surface horizontal plane will be sufficient. For that reason, the following states are defined: $x_D$ and $y_D$ are the positions and $\psi_D$ is the orientation of the diver in the Earth-fixed coordinate frame, while $u_D, v_D$, and $r_D$ are the diver's linear and rotational velocities in the body-fixed frame, respectively. The kinematic model of the diver assumes that the diver cannot swim in the sway direction, i.e., $v_D = 0$ which leads to the kinematic model given with (5), where the diver's rotation matrix $\mathbf{R_D}$ is given with (6).

$$\begin{bmatrix} \dot{x}_D \\ \dot{y}_D \\ \dot{\psi}_D \end{bmatrix} = \begin{bmatrix} \mathbf{R_D}(\psi_D) & \mathbf{0}_{[2\times 1]} \\ 0 & 1 \end{bmatrix} \begin{bmatrix} u_D \\ r_D \end{bmatrix} \tag{5}$$

$$\mathbf{R_D}(\psi_D) = [\cos\psi_D \ \ \sin\psi_D]^T. \tag{6}$$

To enhance the estimation of the diver position, the assumption is made that the diver's surge speed $u_D$ is constant, and the yaw speed $r_D$ has some dynamics determined with a time constant $T_D$. This results in the simplified dynamic model given with (7)

$$\begin{aligned} \dot{u}_D &= 0 \\ \dot{r}_D &= -T_D r_D \end{aligned} \tag{7}$$

### The Tracking Model

The main requirement in the tracking task is to ensure that the distance between the platform and the diver in the horizontal plane $\mathbf{d} = [x - x_D \ \ y - y_D]^T$ converges to zero. The kinematic tracking model is then obtained by differentiation resulting in

$$\dot{\mathbf{d}} = \mathbf{R}(\psi)\begin{bmatrix} u \\ v \end{bmatrix} - \mathbf{R_D}(\psi_D) u_D. \tag{8}$$

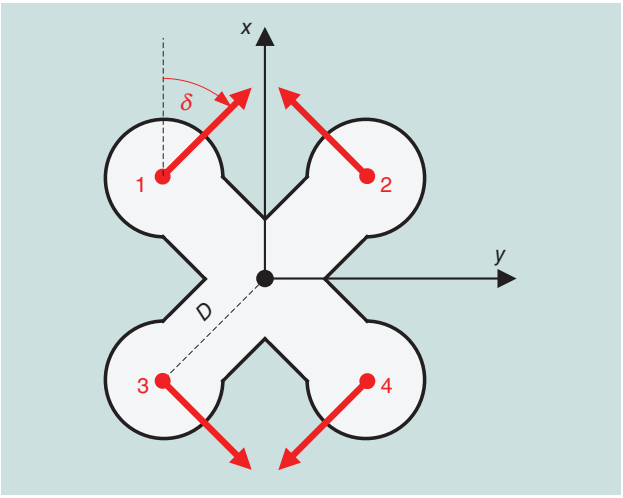


**Figure 6.** The actuator configuration on PlaDyPos. Four thrusters in an X configuration make the vehicle omnidirectional in the horizontal plane.

## Control, Tracking, and Sensor Fusion Algorithms

A control and guidance structure is the most common cascade control structure applied for marine vehicles. The low-level control loop is in charge of speed control and takes the outputs from the upper (guidance) level as its references. Proper tuning of the low-level controllers is a prerequisite for the guidance control-loop tuning [12], whereas, in general, the guidance level is in charge of waypoint following, path and trajectory tracking, and dynamic positioning. For the described application, it is in charge of diver tracking, as shown in Figure 7.

**Diver safety is seriously jeopardized during diving activity.**

### Speed Controller Design

For the low-level speed controller, we have chosen a proportional–integral (PI) controller in the form

$$\boldsymbol{\tau} = \mathbf{K_P}(\boldsymbol{\nu}^* - \boldsymbol{\nu}) + \mathbf{K_I}\int(\boldsymbol{\nu}^* - \boldsymbol{\nu})\,dt + \boldsymbol{\tau}_\mathbf{F}, \tag{9}$$

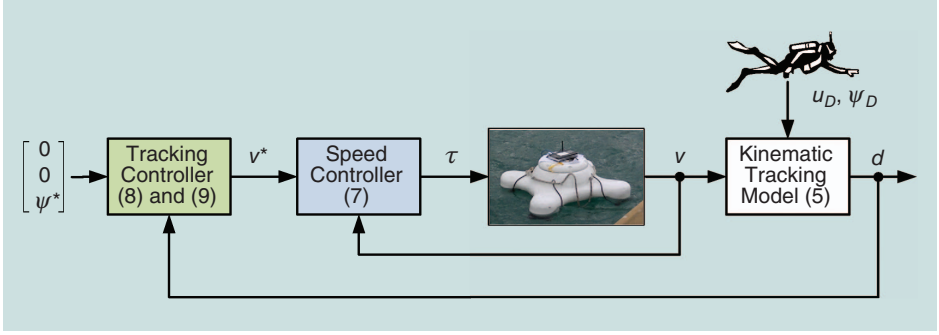


**Figure 7.** The cascade control structure implemented for diver tracking: low-level control is in charge of controlling the surge, sway, and yaw speed, and upper-level control is in charge of generating references for the low-level controllers.

where $\boldsymbol{\nu}^* = [u^* \;\; v^* \;\; r^*]^T$ is the desired linear and angular speeds of the platform, $\mathbf{K_P} = \text{diag}(K_{Pu}, \; K_{Pv}, \; K_{Pr})$ and $\mathbf{K_I} = \text{diag}(K_{Iu}, \; K_{Iv}, \; K_{Ir})$ are diagonal matrices with the PI gains for individual degrees of freedom, respectively. The $\boldsymbol{\tau}_\mathbf{F}$ term represents additional action introduced in the controller to improve the closed-loop behavior. This action can be in the form $\boldsymbol{\tau}_\mathbf{F} = \mathbf{D}(\boldsymbol{\nu})\boldsymbol{\nu}$, which results in the feedback linearization procedure, where measured or estimated speeds are used to compensate for the nonlinearity in the process.

**The diving supervisor at the surface has reliable data about the diver's position, and reliable communication.**

Controller parameters $\mathbf{K_P}$ and $\mathbf{K_I}$ can be calculated based on the desired closed-loop characteristic equation, as shown in [13]. These parameters will naturally depend on the parameters of the dynamic model that have to be identified. The dynamic model parameters of the platform that is addressed in this article have been identified using the identification method based on self-oscillations reported in [14].

### *Guidance Controller Design*

Since the platform is overactuated, it can move in a horizontal plane while keeping an arbitrary heading. For this reason, the high-level guidance controller is divided into the heading controller and the tracking controller design.

#### Heading Controller

For the heading controller, a PI structure is chosen since it compensates for all environmental disturbances in the yaw degree of freedom. In addition, the integral action will compensate for all the unmodeled dynamics and ensure convergence of the heading to the desired value $\psi^*$. The controller can be written in the form

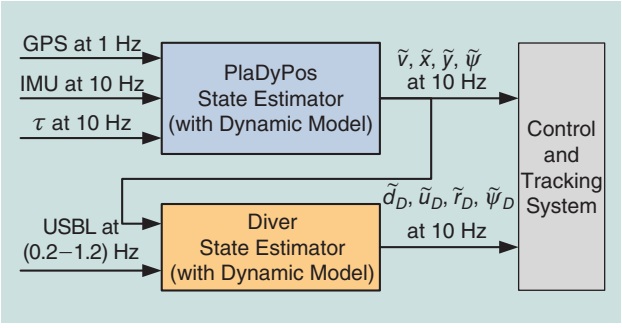


**Figure 8.** A schematic description of estimator inputs and outputs. Since measurements are available at different update rates, the state estimators are used to ensure the update rate of 10 Hz required for the control and tracking system. The diver estimator is also required since diver position measurements are intermittent due to possible occlusions of the acoustic link caused by air bubbles.

$$r^* = K_{P\psi}(\psi^* - \psi) + K_{I\psi}\int(\psi^* - \psi)\,dt, \tag{10}$$

where $K_{P\psi}$ and $K_{I\psi}$ are controller parameters chosen so that the desired heading closed-loop dynamics are achieved.

#### Tracking Controller

With the tracking model given with (8), the PI control action in the form

$$\begin{bmatrix} u^* \\ v^* \end{bmatrix} = \mathbf{R}^{\mathrm{T}}(\psi)\left(-\mathbf{K}_{\mathbf{P},\mathbf{d}}\mathbf{d} - \mathbf{K}_{\mathbf{I},\mathbf{d}}\int \mathbf{d}\,dt\right) + \boldsymbol{\nu}_\mathbf{F}, \tag{11}$$

where $\mathbf{K}_{\mathbf{P},\mathbf{d}} = \text{diag}(K_{P,\text{dx}}, \; K_{P,\text{dy}})$ and $\mathbf{K}_{\mathbf{I},\mathbf{d}} = \text{diag}(K_{I,\text{dx}}, \; K_{I,\text{dy}})$ are PI gain matrices, respectively, will ensure convergence of the distance $\mathbf{d}$ to the desired value $\mathbf{d}^* = [0 \;\; 0]^T$. The $\boldsymbol{\nu}_\mathbf{F}$ is the feedforward action that can improve the behavior of the tracking closed loop. The proposed PI controller will ensure convergence even without the feedforward action, i.e., $\boldsymbol{\nu}_\mathbf{F} = [0 \;\; 0]^T$, [10]. However, tracking may be improved if feedforward action in the form (12) is introduced

$$\boldsymbol{\nu}_\mathbf{F} = \mathbf{R}^T(\psi)\mathbf{R}_\mathbf{D}(\psi_D)\nu_D. \tag{12}$$

The proposed feedforward action requires the estimation of the diver surge speed and heading since they cannot be directly measured.

### *Sensor Fusion*

Two extended Kalman filters are implemented in the system, as shown in Figure 8. Their main purpose is to fuse measurements available at different update rates to ensure state estimations at 10 Hz, as required by the control and tracking system. The PlaDyPos state estimator uses the kinematic (2) and dynamic model (1) of the vehicle to provide speed and position estimates for the control and tracking system based on the input GPS and inertial measurement unit (IMU) measurements as well as the commanded thrust vector $\tau$.

The diver state estimator uses intermittent USBL measurements, PlaDyPos states, and the simplified diver model given with (5) and (7) to estimate tracking distance and speed and orientation of the diver. Since USBL measurements are often not available due to presence of air bubbles exhaled by the diver, this estimator ensures continuous estimates required for the diver-tracking algorithms.

## Benchmark Scenario for Diver Tracking

Performing real-life experiments that include humans and robots is always a complex task. The unpredictability of human nature does not allow replicability of experiments, which is why careful planning and preparation is always required. To validate and replicate diver-tracking experiments under different environmental conditions, we define a benchmark scenario that includes tracking a predefined, georeferenced, and underwater transect. A 50-m rope was laid on seabed at the test site and georeferenced using precise GPS and USBL measurements. During the experiments, the

diver was required to follow the transect in both directions (up and down), with the instructions to deviate as little as possible. While the diver was tracking the transect, the ASV was tracking the diver using the acoustic positioning sensor.

Let $\eta_{\text{PlaDyPos}}$ be the position of the PlaDyPos, while $\eta$ is the measured position, and $\tilde{\eta}$ is the estimated position of a generic agent that is being tracked. We can then define the measure of performance of the tracking system in the form of the mean tracking error given with (13), where $N$ is the number of samples

$$d(\eta) = \frac{1}{N}\sum_{k=1}^{N} \| \eta_{\text{PlaDyPos}}(k) - \eta(k) \|. \tag{13}$$

Similarly, the tracking error for agent position estimates can be defined with $d(\tilde{\eta})$. In the ideal case, this measure should converge to zero, but, due to a number of factors such as modeling uncertainties, measurement errors, and disturbances, this is not the case.

This metric can be used to quantify uncertainties that are present in the human–robot system, given the assumption that the agent is performing perfect tracking. These uncertainties are described in the next section.

## Designing the Experiment

The main goal is to test the diver-tracking capabilities of the system, which is influenced by a number of sources of uncertainties that can compromise repeatability of results. These effects are even more emphasized in the stochastic marine environment. The existence of experimental uncertainties (Table 1), which are difficult and even impossible to model, can be attributed to one of the sources categorized in the following four groups.

Environmental uncertainties include difficult, often impossible to model, influences of wind, waves, and sea currents, whereas environmental influences can be eliminated by performing tests in laboratory conditions, demonstrating the robustness of the performance of the system in the field is a necessity.

Given that the surface vehicle and the diver estimator are described using a simplified model structure with uncertain or changing parameters, unmodeled dynamics present another source of uncertainty that influences repeatability of experiments and the tracking error itself. This category includes also uncertainties inherent to mechanical components, unpredictable faults that can occur (most often in actuators), and basic navigation sensors onboard mobile robots, such as the compass, the GPS, and the IMU.

**Conducting experiments with divers presents a challenge due to uncertainties.**

Acoustic sensor uncertainties are most emphasized in the acoustic communication and positioning system, and they are caused by complex acoustic channel parameters, such as water temperature and salinity. Additional effects that compromise acoustic channel include multipath effects and update rates that vary depending on the acoustic channel information payload size. The accuracy of the used sensor is specified in [15] as ±0.2 m in range calculation and ±3° for bearing and elevation measurements. This accuracy analysis comes from a nearly static scenario with precise calibration and good acoustic channel conditions without multipath or air bubble interference. At a 10-m distance, the expected position noise would therefore be around ±0.5 m. Given that the USBL is mounted on a mobile platform (under the influence of waves during experiments) and the modem is mounted on the mobile agent, additional performance degradation of the acoustic

**Table 1. A summary of the most significant uncertainties in the experimental setups.**

| | Setup | | | |
|---|---|---|---|---|
| **Source of Uncertainties** | 0 | 1 | 2 | 3 |
| Environmental disturbances | – | ✓ | ✓ | ✓ |
| Unmodeled dynamics | – | ✓ | ✓ | ✓ |
| Acoustic sensor | – | – | ✓ | ✓ |
| Diver influence | – | – | – | ✓ |

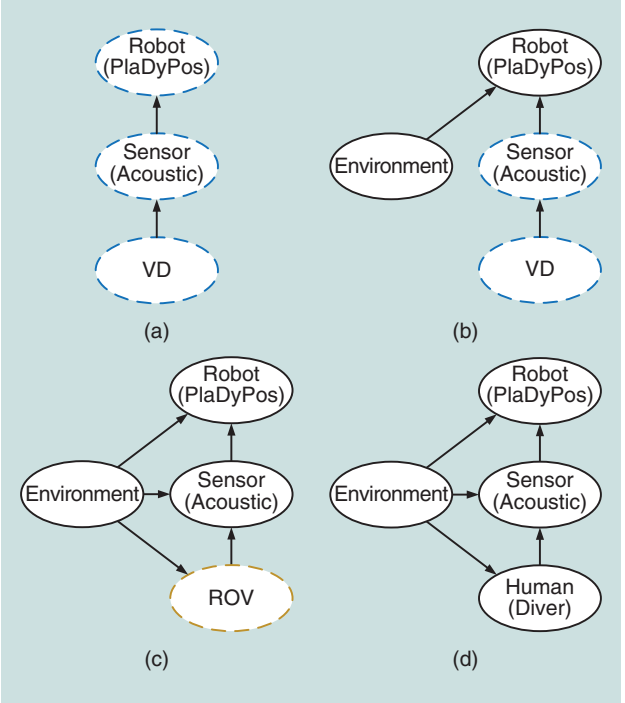


**Figure 9.** A schematic description of experimental setups: (a) setup 0, (b) setup 1, (c) setup 2, and (d) setup 3. The blue dashed lines represent simulated segments. Setup 0 is pure simulation. Setup 1 includes real ASV operating in the environment with a simulated diver and acoustic channels to eliminate uncertainties introduced by the acoustic sensor and the human diver. Setup 2 introduces acoustic sensor uncertainty by utilizing a manually controlled ROV connected to the ASV via an acoustic link, while setup 3 includes the diver uncertainties in the experiment.

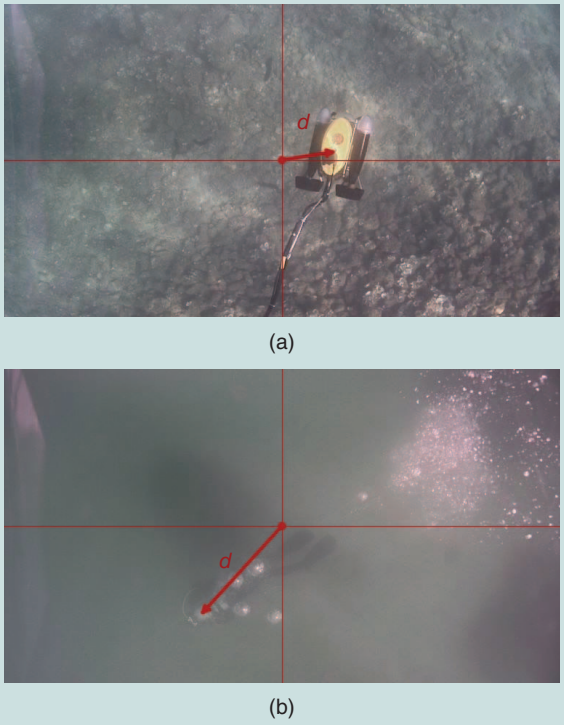


**Figure 10.** The visual ground truth of the obtained results: (a) a video still from experimental setup 2 and (b) a video still from experimental setup 3. The ROV and the diver are detected in video images, and their distance to the image center is determined as the true tracking error. Note the bubble clouds that may obstruct the acoustic channel.

sensor compared with the nominal accuracy specifications is expected.

**The diver's area of operation can be increased if the diving buoy is linked to the diver via a cable.**

The greatest source of uncertainty is definitely the human diver. Even though the diver can be instructed to execute preplanned missions required in an experiment, there is always the issue of bubble emission, due to breathing, which may obstruct the communication channel. In addition to that, diver motion can cause different positioning of the modem relative to the USBL, influencing the quality of the acoustic communication and sometimes causing obstruction of the acoustic line of sight.

To perform the structured experiments with the diver, a step-by-step experimental plan is designed to examine the influence of the abovementioned uncertainties.

### *Setup 0 Simulation Experiments [Figure 9(a)]*

Both the surface vehicle and the diver are simulated to test the implemented algorithms for errors and to determine the best possible performance of the diver-tracking system. This step naturally eliminates any type of uncertainty.

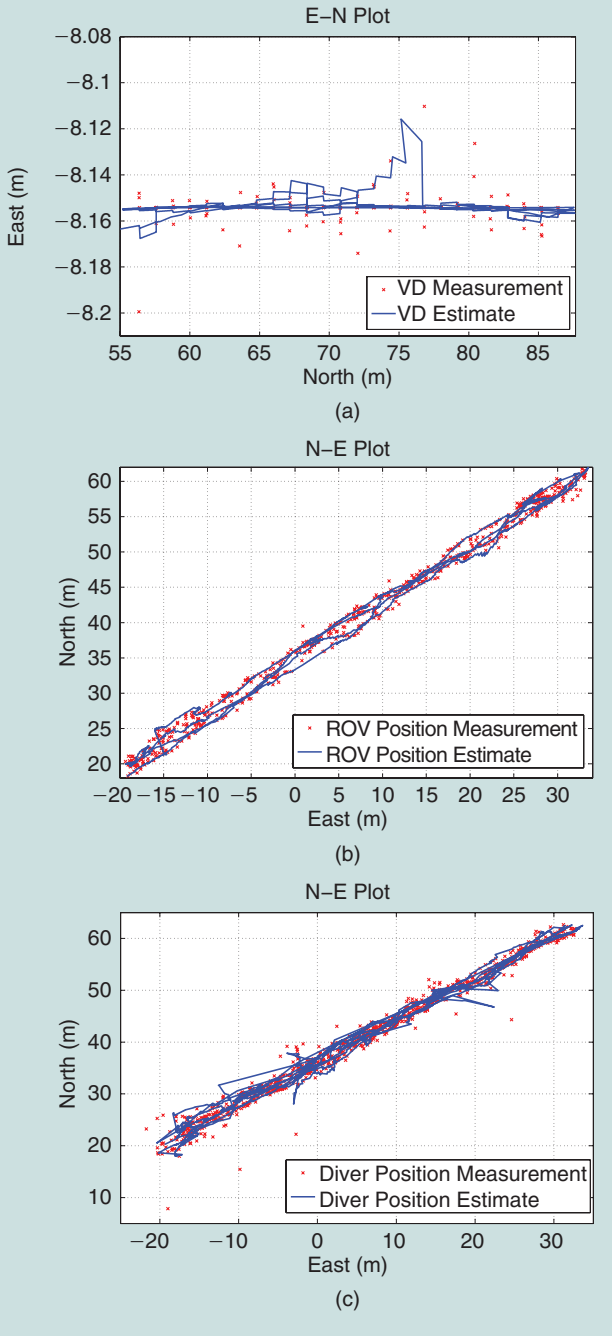


**Figure 11.** The position plots of tracked agents (VD, ROV, and human diver) during transect following in all conducted experiments. The red asterisks indicate the intermittent and noisy raw USBL measurements, while the blue lines show estimates of the positions based on the diver kinematic and dynamic model. Under the assumption that the agents were tracking the transect with little lateral deviation, variation of the measured and estimated positions in three experimental setups indicate the influence of different uncertainties. (a) Setup 1: VD and PlaDyPos. (b) Setup 2: ROV and PlaDyPos. (c) Setup 3: diver and PlaDyPos.

### *Setup 1 VD and PlaDyPos [Figure 9(b)]*

The platform, placed in a real environment, tracks the VD that is simulated using a simple mathematical model given

with (7). While this experimental setup eliminates acoustic sensor and diver related uncertainties, it also allows reliable testing of PlaDyPos behavior under different measurement update rates and performance evaluation of the diver estimator onboard PlaDyPos in real environmental conditions.

### *Setup 2 ROV and PlaDyPos [Figure 9(c)]*

In this real-environment setup, the human diver is replaced with an ROV with an acoustic modem pinging the USBL on the PlaDyPos, and thus introducing the real acoustic channel uncertainties but eliminating those caused by the diver. This setup is designed to identify potential deterioration in system performance due to the acoustic channel characteristics.

### *Setup 3 Diver and PlaDyPos [Figure 9(d)]*

The final experimental setup, which is in fact the demonstrator of the final goal of the described robotic system, includes experiments in real conditions with all the abovementioned uncertainties included.

To validate the results, a visual confirmation that gives a ground truth of the tracking performance is made. A down-looking camera was mounted on the PlaDyPos to validate the tracking results for setups 2 and 3 (where real agents are being tracked). Position of the agent is determined within the image, and its distance to the center of the image is calculated in pixels. Based on the known size of the ROV and the diver, the measure in pixels is transferred to meters, giving ground truth of the tracking performance. Influence of the roll and pitch of PlaDyPos is compensated using the measurements from the inertial sensor. An example of the images obtained from the two setups is shown in Figure 10.

The accuracy of the vision-based ground truth can be compromised if the camera orientation is not perfectly aligned with the gravity vector. The upper limit of the error in the observed position of the agent $\Delta x$ can be estimated by using a simplified model $\Delta x = z \cdot \tan\alpha$, where $z$ is the depth of the agent and $\alpha$ is the camera orientation with respect to the gravity vector. If the misalignment is not larger that $\alpha = 5^{\circ}$, the estimate of upper limit of the error is less than 10% of the depth of the agent.

## Experimental Results

A large number of experiments, with previously described experimental setups, were conducted in June 2014 in Split, Croatia, at the Croatian Navy base. Position plots of all obtained results with a VD, ROV, and a human diver during transect following in three experimental setups are shown in Figure 11. Even in these position plots, it can be seen that the variance of measurements depends on the experimental setup, from low variance in experiments with the VD to high variance in experiments with the human diver due to a large number of sources of uncertainty.

To get a clearer picture of the influence of different sources of uncertainty on the tracking error, results from each experimental setup are analyzed. Simulation results from setup 0 are omitted from this article to keep the focus on results obtained in real environmental conditions. The simulation results can be found in [10].

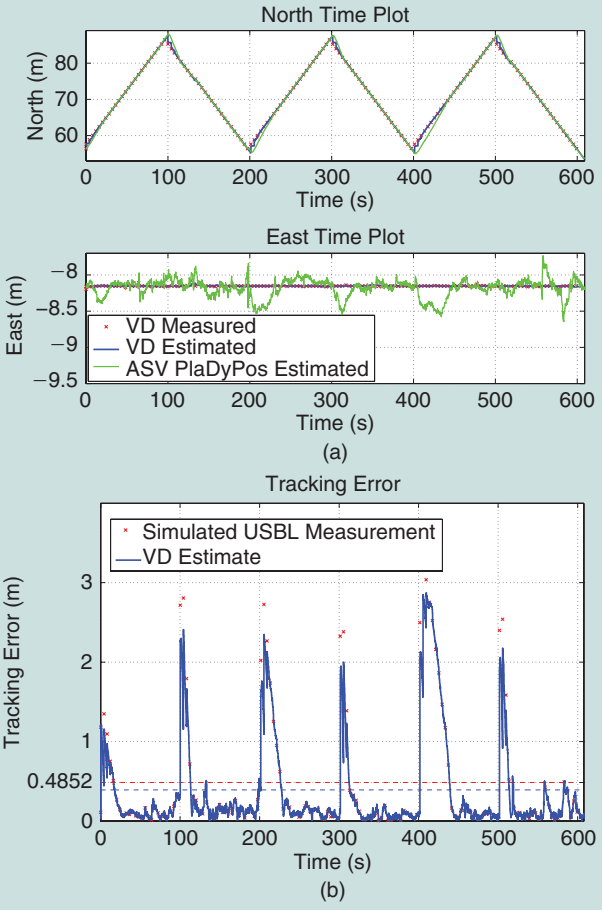


**Figure 12.** The experimental results obtained from setup 1 with the VD: (a) the north and east positions and (b) the tracking error. The largest tracking errors are due to abrupt changes in the direction of the VD. The diver position is estimated from the measurements with great precision, and a smooth signal is ensured for the tracking system at frequency higher than the measurement availability.

**Table 2. Metric for the uncertainties: mean tracking errors of agents (VD, ROV, human diver).**

| | Mean Tracking Error in (m) | | |
|---|---|---|---|
| | $d(\eta)$ | $d(\tilde{\eta})$ | From Video |
| Setup 1 ($\eta = \eta_{\text{virtual diver}}$) | 0.4852 | 0.3906 | — |
| Setup 2 ($\eta = \eta_{\text{ROV}}$) | 0.9994 | 0.4512 | 0.9169 |
| Setup 3 ($\eta = \eta_{\text{diver}}$) | 1.7772 | 1.3510 | 1.4831 |

### *Results for Setup 1: VD Tracking*

The full experiment with the VD tracking in duration of about 10 min is shown in Figure 12. While the results given in Figure 12(a) indicate that PlaDyPos was following the same path as the VD, the real VD tracking quality is observed from

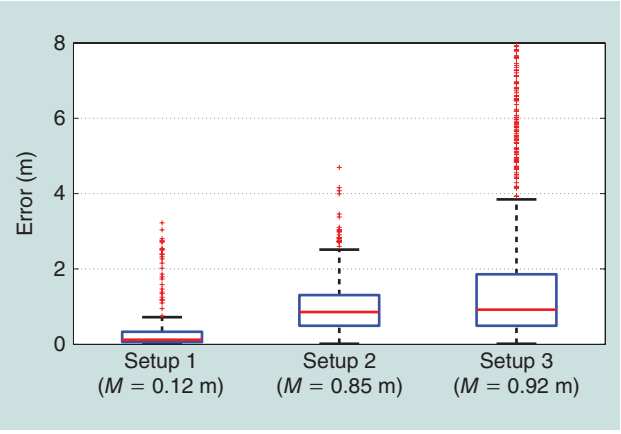


**Figure 13.** The distribution of the measured tracking errors for all setups. Note that for setups 2 and 3 the median tracking error ($M$) is similar since the same sensor is used. However, diver effects in setup 3 are manifested with a higher spread of tracking errors and a larger number of outliers.

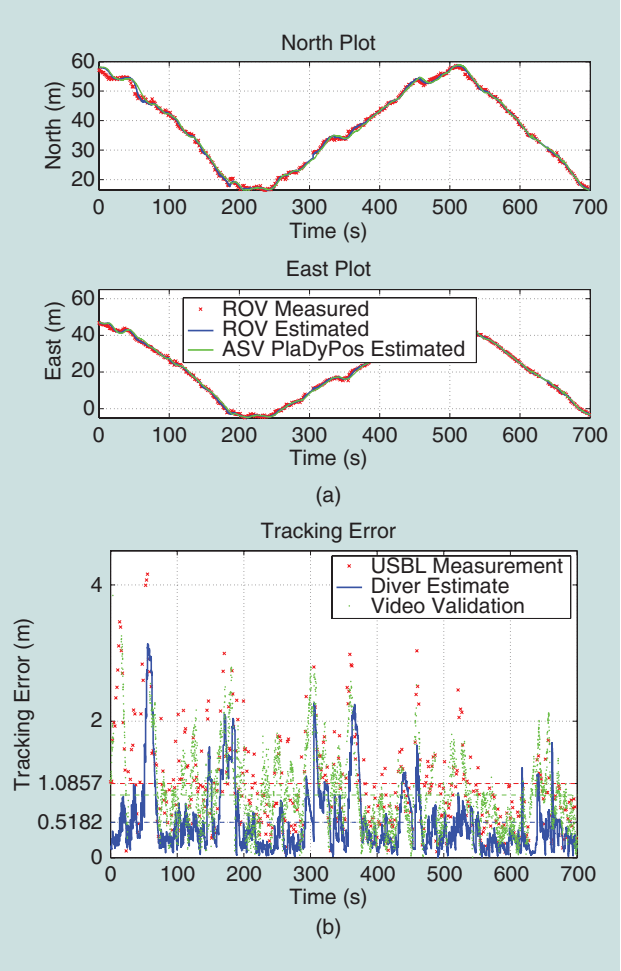


**Figure 14.** The experimental results obtained from setup 2 with the ROV replacing the human diver: (a) the north and east positions and (b) the tracking error. The tracking error during the experiment shows satisfactory behavior even when real acoustic measurements (red asterisk) are used. The overlayed ground-truth video validation shows that the ROV estimator is providing ROV position estimates in line with true ROV position. Horizontal dashed lines denote mean tracking error during the presented segment of the experiment while Table 2 contains values for the experiment.

Figure 12(b). By applying (13), the mean tracking error using both measured diver positions and the estimates is shown in Table 2. Since this experimental setup is influenced only by the environmental disturbances and uncertainties caused by unmodeled dynamics, we conclude that these uncertainties cause the mean error of about 0.5 m. The error distribution, shown in Figure 13, indicates an error median of about 0.12 m with the majority of tracking errors below 1 m with a smaller number of statistical outliers.

This error is mostly due to transients that occur when the VD is changing the direction of transect following, as shown in Figure 12(b).

### *Results for Setup 2: ROV Tracking*

The second experimental setup is designed to determine the influence of the acoustic positioning system in the diver-tracking scenario. Even though multiple experiments were performed [see Figure 11(b)], the results in Figure 14 show only 10 min of the experiment, for the sake of clarity.

Table 2 shows that the mean tracking error based on acoustic measurements in this setup is about 1 m, which lets us conclude that the inclusion of the acoustic sensor uncertainty increases the tracking error by 0.5 m. Observe the same increase in Figure 13, where the sensor uncertainty increased the median tracking error to around 0.85 m. The number of outliers did not increase, but the measured tracking errors are more spread than in setup 1.

### *Results for Setup 3: Diver Tracking*

Finally, setup 3 allows us to quantify the influence of the human diver. Diver-tracking results obtained from one single transect coverage in upward and downward direction are shown in Figure 15.

It can be seen in the initial part of the experiment how PlaDyPos is converging above the diver. At around 290 s, Figure 15(a) shows the system behavior in situations when USBL measurements are not available for a longer period of time due to acoustic channel occlusion caused by the diver uncertainties. The estimator keeps providing the estimated diver position, and PlaDyPos tracks this estimate. Almost 30 s later, the measurements are again available, and the estimated diver position converges to the measured diver position, together with the position of PlaDyPos, ensuring high quality tracking. It should be mentioned that the diver position estimator is satisfactory for shorter periods of measurement unavailability. The specific case of more than 30 s without measurements shows that diver motion cannot be estimated for a longer period of time. The tracking error during the experiment is shown in Figure 15(b). It can be seen that, apart from the initial convergence phase and the phase when the measurements were not available, the error based on measurements is almost always below 2 m and the error based on diver estimates is below 1 m.

Mean tracking errors for all experiments with the divers are shown in Table 2, not only the single transect shown in Figure 15. The mean tracking error based on the measurements, compared

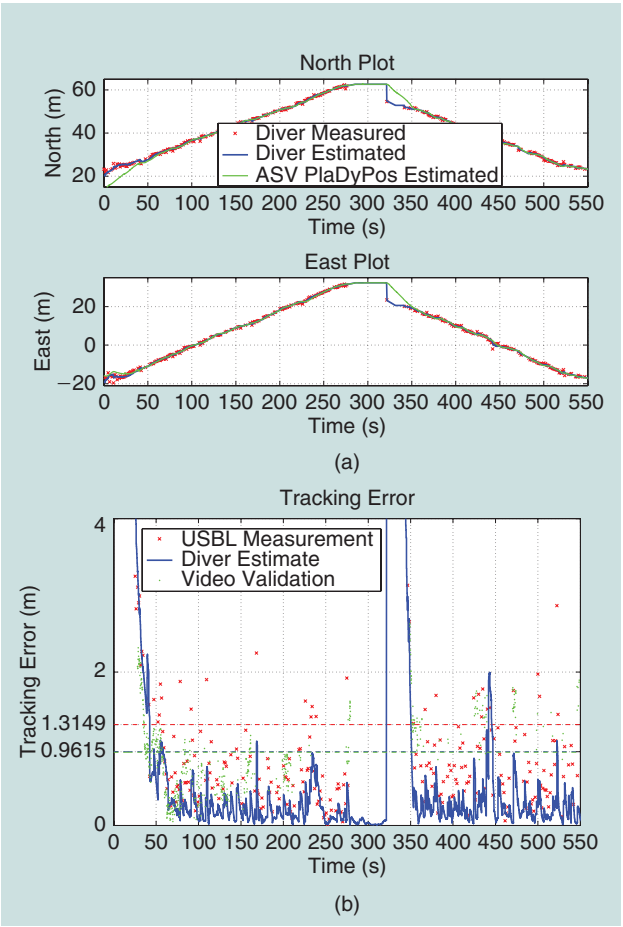


**Figure 15.** The experimental results obtained from setup 3 with the human diver: (a) the north and east positions and (b) the tracking error. A long period of missing acoustic data is visible at around 300 s—the diver position estimator provides estimates based on a simplified diver model during this period and during other, shorter, periods when measurements are not available. The overlayed ground-truth video validation shows that the diver estimator is providing estimates in line with true diver position. Horizontal dashed lines denote mean tracking error during the presented segment of the experiment, while Table 2 contains values for the complete experiment.

with the result from setup 2, allows us to conclude that the presence of the human diver contributes an additional 0.8 m resulting in the total error of about 1.8 m. The tracking error calculated based on the diver position estimates is considerably lower. Observe that the presence of the human diver has little influence on the median measured tracking error, as shown in Figure 13. However, the increase of statistical outliers and the higher spread are attributed to the diver's presence.

### *Ground-Truthing the Results*

Since during the experiment both the diver and the ROV were tracking the transect at a depth of about 5 m, it was possible to detect them in the video image. The accuracy of the visual ground truth is estimated to about ±0.5 m based on the error estimation analysis (due to misalignment of the camera with the gravity vector) provided before. It should be mentioned that at larger depths this type of validation would not be possible due to low visibility.

The tracking error based on video data is overlayed in Figures 14(b) and 15(b), and the mean tracking error values are listed in Table 2. These values are very close to the measured and the estimated mean tracking errors showing the accuracy of the results obtained from measured and estimated positions. It should also be mentioned that the difference between the setups 2 and 3 mean tracking error from video data is around 0.6 m, which shows that the influence of the human uncertainty determined by the acoustic measurements (0.8 m) and the estimated diver positions (0.9 m) are sufficiently accurate.

The mean error from the diver position estimates is lower due to inclusion of the diver estimator. However, it should be mentioned that if this error is too conservative, the diver motion is not estimated properly. By comparing this estimation with the video validation, we conclude that the diver estimator gives satisfactory results.

## Open Data

The experiment described in this article was designed to allow future replication for comparison with new positioning sensors and methods. All software was implemented within the ROS (http://www.ros.org) framework which is used by the worldwide robotics community. During the experiments, all the relevant data were logged in an ROS bag format. Video validation footage was time stamped and logged into a separate ROS bag file due to its size. An a posteriori analysis of the experimental data was performed to identify and extract parts where actual tracking has taken place. Filtered bag files were loaded into MATLAB where the final analysis step was performed. The data and MATLAB scripts used during analysis are made publicly available at https://bitbucket.org/labust/diver-tracking, together with clear instructions on how to use the data. Making the data and scripts available in a Git repository makes future changes and contributions easily trackable.

**The diver state estimator uses intermittent USBL measurements, PlaDyPos states, and simplified diver model.**

## Conclusions

The benchmark scenario of following a georeferenced transect laid on the seabed allowed us to execute replicable experiments with an ASV for diver tracking. Given that experiments with human divers introduce a large number of uncertainties, a structured step-by-step experimental plan was devised with the intention to identify the influence of uncertainties introduced by the environment, the unmodeled dynamics, the acoustic sensors, and the human diver. We have defined a metric in the form of a mean tracking

error that allowed us to quantify influences of different uncertainties.

The results obtained using the surface vehicle tracking a VD have shown that the mean tracking error is around 0.5 m. When an ROV was used instead of the VD, uncertainties caused by the acoustic sensor were introduced, and the mean tracking error increased to around 1 m. In the final step, human diver and experimental uncertainties related to human factors (such as bubble emission) were introduced, significantly increasing the mean tracking error to 1.8 m.

**Two extended Kalman filters are implemented in the system, as shown in Figure 8.**

The obtained data was validated against the ground-truth data provided by the video stream from which the distance of the ROV and the diver from the surface vehicle was determined. The obtained results confirmed the tracking quality attained from the experiments using the acoustic positioning device, and proved the accuracy of the diver-tracking system.

There is a large number of parameters in the control, tracking, and estimation system that can be tuned, and a large number of control, tracking, and estimation methods that can be implemented. All the obtained data and code are made available online for public use. The results provided in this article are set as a benchmarking performance and it is left to the whole interested community to compare, analyze, and improve the performance of the diver-tracking system by using different algorithms, sensors, and vehicles.

## Acknowledgment

The authors would like to thank the Croatian Navy for securing the trial area and providing logistic support, and Nikola Stilinović, Milan Marković, Filip Mandić, and Antonio Vasilijević for their assistance during the execution of the experiments.

This work was supported by the European Commission under the Seventh Framework Program project "CADDY—Cognitive Autonomous Diving Buddy" under Grant Agreement 611373 and by the Business Innovation Agency of the Republic of Croatia through the Proof of Concept Program.

## References

[1] D. Schories and G. Niedzwiedz. (2012). Precision, accuracy, and application of diver-towed underwater GPS receivers. *Environ. Monitoring Assessment*. [Online]. *184(4)*. pp. 2359–2372. Available: http://www.scopus.com/inward/record.url?eid=2-s2.0-84862885600&partnerID=40&md5=f6ff96e3dc1e4c14fea3db111ff4e71d

[2] M. Stojanovic and J. Preisig, "Underwater acoustic communication channels: Propagation models and statistical characterization," *IEEE Commun. Mag.*, vol. 47, no. 1, pp. 84–89, Jan. 2009.

[3] C. Georgiades, A. German, A. Hogue, H. Liu, C. Prahacs, A. Ripsman, R. Sim, L.-A. Torres, P. Zhang, M. Buehler, G. Dudek, M. Jenkin, and E. Milios, "AQUA: An aquatic walking robot," in *Proc. IEEE/RSJ Int. Conf. Intelligent Robots Systems*, Sept. 2004, vol. 4, pp. 3525–3531.

[4] G. Dudek, M. Jenkin, C. Prahacs, A. Hogue, J. Sattar, P. Giguere, A. German, H. Liu, S. Saunderson, A. Ripsman, S. Simhon, L.-A. Torres, E. Milios, P. Zhang, and I. Rekletis, "A visually guided swimming robot," in *Proc. IEEE/RSJ Int. Conf. Intelligent Robots Systems*, Aug. 2005, pp. 3604–3609.

[5] A. Birk, G. Antonelli, A. Caiti, G. Casalino, G. Indiveri, A. Pascoal, and A. Caffaz, "The CO$^3$AUVs (cooperative cognitive control for autonomous underwater vehicles) project: Overview and current progresses," in *Proc. IEEE OCEANS—Spain*, June 2011, pp. 1–10.

[6] T. Glotzbach, M. Bayat, A. Aguiar, and A. Pascoal. (2012). An underwater acoustic localisation system for assisted human diving operations. in *Proc. IFAC Volumes (IFAC-PapersOnline)*. pp. 206–211. [Online]. Available: http://www.scopus.com/inward/record.url?eid=2-s2.0-84900508038&partnerID=40&md5=7c2bd2f8cc0f458a7df48f85066d188e

[7] K. Demarco, M. West, and A. Howard. (2013). A simulator for underwater human-robot interaction scenarios. in *Proc. MTS/IEEE OCEANS: An Ocean in Common—San Diego*. [Online]. Available: http://www.scopus.com/inward/record.url?eid=2-s2.0-84896345210&partnerID=40&md5=9ca2ba614e5b3ce83f31f0f20ad68da9

[8] H. Buelow and A. Birk, "Diver detection by motion-segmentation and shape-analysis from a moving vehicle," in *Proc. IEEE OCEANS*, Sept. 2011, pp. 1–7.

[9] K. DeMarco, M. West, and A. Howard, "Sonar-based detection and tracking of a diver for underwater human-robot interaction scenarios," in *Proc. IEEE Int. Conf. Systems, Man, Cybernetics*, Oct. 2013, pp. 2378–2383.

[10] N. Miskovic, D. Nad, N. Stilinovic, and Z. Vukic, "Guidance and control of an overactuated autonomous surface platform for diver tracking," in *Proc. 21st Mediterranean Conf. Control Automation (MED)*, 2013, pp. 1280–1285.

[11] T. Fossen, *Guidance and Control of Ocean Vehicles*. New York: Wiley, 1994.

[12] N. Mišković, M. Bibuli, G. Bruzzone, M. Caccia, and Z. Vukić, "Tuning marine vehicles' guidance controllers through self–oscillation experiments," in *Proc. 8th IFAC Int. Conf. Manoeuvring Control Marine Craft (MCMC)*, 2009, pp. 115–120.

[13] M. Caccia, M. Bibuli, R. Bono, and G. Bruzzone, "Basic navigation, guidance and control of an unmanned surface vehicle," *Auton. Robot.*, vol. 25,no. 4, pp. 349–365, 2008.

[14] N. Miskovic, Z. Vukic, M. Bibuli, G. Bruzzone, and M. Caccia, "Fast in-field identification of unmanned marine vehicles," *J. Field Robot.*, vol. 28, no. 1, pp. 101–120, 2011.

[15] A. Vasilijevic, B. Borovic, and Z. Vukic, "Underwater vehicle localization with complementary filter: Performance analysis in the shallow water environment," *J. Intell. Robot. Syst.*, vol. 68, nos. 3–4, pp. 373–386, 2012.

***Nikola Mišković***, University of Zagreb, Faculty of Electrical Engineering, Zagreb, Croatia. E-mail: nikola.miskovic@fer.hr.

***Đula Nađ***, University of Zagreb, Faculty of Electrical Engineering, Zagreb, Croatia. E-mail: dula.nad@fer.hr.

***Ivor Rendulić***, University of Zagreb, Faculty of Electrical Engineering, Zagreb, Croatia. E-mail: ivor.rendulic@fer.hr.